 DOI: 10.1002/eji.201545789 Eur. J. Immunol. 2016. 46: 192–203

European Journal of Immunology

Depletion of CD11c$^+$ cells in the CD11c.DTR model drives expansion of unique CD64$^+$ Ly6C$^+$ monocytes that are poised to release TNF-α

Shivajanani Sivakumaran[*1,2], *Stephen Henderson*[*2,3], *Sophie Ward*[1,2], *Pedro Santos E. Sousa*[1,2], *Teresa Manzo*[1,2], *Lei Zhang*[1,2], *Thomas Conlan*[1,2], *Terry K. Means*[4], *Maud D'Aveni*[5], *Olivier Hermine*[5], *Marie-Thérèse Rubio*[5], *Ronjon Chakraverty*[**1,2] and *Clare L. Bennett*[**1,2]

[1] Institute for Immunity and Transplantation, University College London, London, UK
[2] Cancer Institute, University College London, London, UK
[3] Bill Lyons Informatics Centre, University College London, London, UK
[4] MGH Center for Immunology and Inflammatory Diseases, Harvard Medical School, Boston, MA, USA
[5] CNRS UMR 8147, Université Paris Descartes, Faculté de Médecine, Hôpital Necker, Paris, France

Dendritic cells (DCs) play a vital role in innate and adaptive immunities. Inducible depletion of CD11c$^+$ DCs engineered to express a high-affinity diphtheria toxin receptor has been a powerful tool to dissect DC function in vivo. However, despite reports showing that loss of DCs induces transient monocytosis, the monocyte population that emerges and the potential impact of monocytes on studies of DC function have not been investigated. We found that depletion of CD11c$^+$ cells from CD11c.DTR mice induced the expansion of a variant CD64$^+$ Ly6C$^+$ monocyte population in the spleen and blood that was distinct from conventional monocytes. Expansion of CD64$^+$ Ly6C$^+$ monocytes was independent of mobilization from the BM via CCR2 but required the cytokine, G-CSF. Indeed, this population was also expanded upon exposure to exogenous G-CSF in the absence of DC depletion. CD64$^+$ Ly6C$^+$ monocytes were characterized by upregulation of innate signaling apparatus despite the absence of inflammation, and an increased capacity to produce TNF-α following LPS stimulation. Thus, depletion of CD11c$^+$ cells induces expansion of a unique CD64$^+$ Ly6C$^+$ monocyte population poised to synthesize TNF-α. This finding will require consideration in experiments using depletion strategies to test the role of CD11c$^+$ DCs in immunity.

Keywords: CD11c.DTR · Dendritic cells · Depletion · Diphtheria toxin receptor (DTR) · Monocytes · Monocytosis

Additional supporting information may be found in the online version of this article at the publisher's web-site

Correspondence: Dr. Clare L. Bennett
e-mail: c.bennett@ucl.ac.uk

*These authors contributed equally to this work.
**These authors are joint senior authors.

Introduction

Dendritic cells (DCs) play a vital role in the activation and control of cellular immunity. Much of our understanding of the requirement for DCs in regulating immunity has come from in vivo models of DC depletion in which different DC populations are engineered to express a high-affinity diphtheria toxin (DT) receptor (DTR), and can be inducibly and transiently depleted in vivo upon injection of DT [1, 2]. Inducible cell ablation is a powerful tool to understand the role of a population of cells in vivo. However, it is important that conclusions made regarding the physiological functions of DCs following experimental depletion are also informed by the impact that depletion has upon other cells in the immune system.

Bone marrow (BM) derived circulating monocytes can be divided into two populations, which are distinguished in mice by expression of the glycoprotein Ly6C [3, 4]. "Nonclassical" Ly6C^{neg} monocytes patrol endothelial vessels in the steady state and are positioned to initiate a rapid response to infection [5]. "Classical" or "inflammatory" Ly6C^{+} monocytes are released from the BM via ligation of the chemokine receptor CCR2 [6–8]. The recent identification of a common monocyte progenitor (cMoP) [9] and lineage-tracing studies suggest a linear model in which cMoPs give rise to Ly6C^{+} cells, which in turn seed the Ly6C^{neg} pool [4, 10]. Activation of Ly6C^{+} monocytes results in the upregulation of molecules associated with macrophage and DC function, and classical monocytes were long thought to function as a pool of rapid reactionary cells capable of augmenting tissue DCs and macrophages during inflammation [11–14]. However, a number of recent studies have now demonstrated that Ly6C^{+} monocytes directly participate in innate and adaptive immunities [15–18], and in the absence of infection, monocytes extravasate into tissues and may contribute to immunosurveillance of peripheral antigens [19, 20]. Migration across the vascular endothelium into tissue is sufficient to induce upregulation of molecules such as the high-affinity IgG receptor FcγRI (CD64), and is linked to transition toward a more activated and/or differentiated cell type [20, 21].

The relative proportion of monocytes within the steady-state mononuclear phagocyte system (MPS) is finely controlled by serum levels of myeloid growth factors such as M-CSF, G-CSF, and fms-like tyrosine kinase receptor-3 (ligand, Flt3(L)) [22]. This balance has been exemplified in studies using the constitutive and transient depletion of DCs. CD11c.DTA mice that are born lacking DCs develop a myeloproliferative syndrome by 3 months of age due to enhanced extramedullary hematopoiesis in the spleen resulting in accumulation of CD115^{+} monocytes [23]. Homeostasis of DC populations depends on signaling via Flt3, and removal of DCs results in increased serum levels of Flt3(L) [23–25]. The increase in Flt3(L) drives myeloproliferation in DC-deficient animals, due to the direct stimulation of myeloid progenitors in the spleen [23]. Similarly, transient loss of DCs from DC-specific DTR mice also induces monocytosis [2, 23, 26–28]. However, despite reports of enhanced numbers of monocytes in DC-depleted mice the immune characteristics of these cells have not been investigated.

In this study, we find that transient depletion of CD11c^{+} cells from CD11c.DTR mice results in the CCR2-independent, G-CSF-dependent expansion of a novel CD64^{+} Ly6C^{+} monocyte population in the spleen that is transcriptionally distinct from both Ly6C^{+} and Ly6C^{neg} monocytes. This variant monocyte population is poised to release TNF-α on stimulation with LPS, and has the potential to mediate inflammatory immunity in the absence of DCs.

Results

Depletion of CD11c^{+} cells leads to expansion of a distinct population of CD64^{+} Ly6C^{+} monocytes

To investigate the effect of depletion of CD11c^{+} DCs on the MPS, we injected CD11c.DTR/EGFP mice with a single dose of DT or PBS, and analyzed myeloid cells in the spleen 48 h later. Supporting Information Figure 1 shows that CD11c^{high} GFP^{+} DCs are efficiently ablated from the spleen in this model, along with CD11b^{+}F4/80^{+}Ly6C^{low} macrophages as has been previously reported [28, 29]. Other nonmyeloid immune populations were not affected (Supporting Information Fig. 1C). Analysis of splenocytes from DT-treated recipients demonstrated that depletion of CD11c^{+} cells resulted in the expansion of two populations of granular side scatter (SSC)$^{int\ to\ high}$ CD11b^{+} myeloid cells, in accord with published data [26, 30, 31], that differentially expressed Ly6C (Fig. 1A). Further, flow cytometric analyzes defined SSC^{int} cells as Ly6C^{high}CD115^{high} classical monocyte-like cells (referred to as Ly6C^{+} monocytes). The second SSC^{high} population was designated CD11b^{+}Ly6C^{+}CD115^{int} neutrophils, which were further defined by expression of Ly6G (Fig. 1A and B). Staining with Ly6G also highlighted the presence of an uncharacterized population of Ly6G^{neg} Ly6C^{int} cells in DT-treated mice (Fig. 1A). Kinetic analyzes demonstrated that the increase in splenic Ly6C^{+} monocytes peaked 2 days after the injection of DT and decreased by day 4 (Fig. 1C). We also observed a concurrent peak in the number of splenic neutrophils (Supporting Information Fig. 2A). However, in the blood and BM, monocytes continued to expand over the course of the experiment (Fig. 1D). By contrast, the frequency of neutrophils rapidly increased in the blood and BM 1 day after treatment. This increase was not matched by a change in the numbers of BM neutrophils, possibly due to small differences in the frequency of BM neutrophils in the context of other changing cell populations (Supporting Information Fig. 2B). The increases in splenic monocytes and neutrophils were also confirmed by analyzing expansion of CD11b^{+}Ly6C^{+} and Ly6G^{+} cells, respectively, 48 h after the injection of PBS or DT (Supporting Information Fig. 2C). To confirm that expansion of Ly6C^{+} cells was dependent on depletion of CD11c-expressing cells, we injected DT into both wild-type (WT) C57BL/6 mice and Langerin.DTR mice, the latter another DTR expressing strain, and analyzed the expansion of

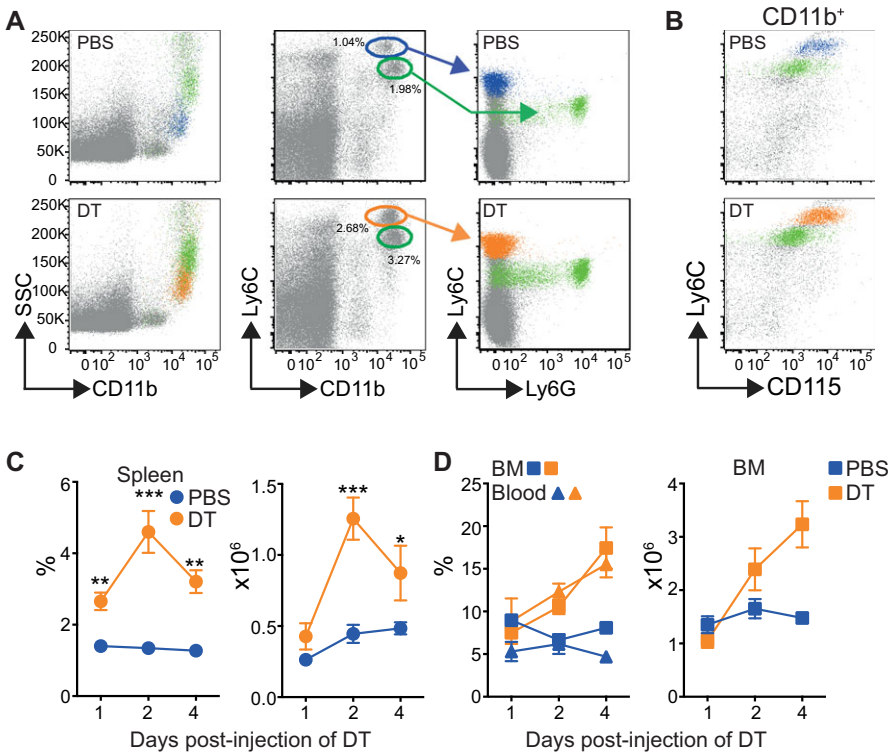

Figure 1. Expansion of Ly6C$^+$ monocytes following depletion of CD11c$^+$ cells. CD11c.DTR mice were injected with PBS or DT and analyzed 48 h later. (A) Representative dot plots showing the expansion of monocytes (blue and orange) and neutrophils (green) in the spleens of PBS- and DT-injected CD11c.DTR mice. Dot plots are pregated on live single cells. Dot plots on the far right show expression of Ly6C and Ly6G by CD11b$^+$Ly6C^{high} (blue and orange) and CD11b$^+$Ly6C^{int} (green) gated cells overlaid on live cells. (B) Representative dot plots showing expression of CD115 and Ly6C by gated CD11b$^+$Ly6C^{high} (blue and orange) or Ly6C^{int} (green) cells. Plots are representative of more than three independent experiments. (C) Graphs show the percentage ± SEM (left) and number ± SEM (right) of CD11b$^+$Ly6C^{high} monocytes in the spleen of PBS-treated (blue) and DTR-treated (orange) recipients at different times post injection of DT. Two-way ANOVA with multiple comparisons (*) PBS versus DT on day 2 $p < 0.0001$. Data are pooled from multiple independent experiments: day 1 PBS/DT $n = 6$, day 2 PBS/DT $n = 26/24$, day 4 PBS/DT $n = 6$. (D) Left: graph showing the frequency ± SEM of monocytes in the blood and BM of PBS-treated (blue triangles and squares) and DT-treated (orange triangles and squares) recipients. Two-way ANOVA with multiple comparisons (*) day 2 BM and blood $p = 0.0016$ and $p = 0.0012$, respectively, day 4 $p < 0.0001$ for both. Right: graph showing the number ± SEM of monocytes in the BM from the femurs and tibias of one back leg. Two-way ANOVA with multiple comparisons (*) $p = 0.0015$ on day 4. Data are pooled from multiple independent experiments: days 1 and 4 PBS/DT $n = 6$, day 2 BM PBS/DT $n = 14/12$, blood PBS/DT $n = 12$.

Ly6C$^+$ cells in the spleen 48 h later. Ly6C$^+$ cells did not expand in the spleen or epidermis of either DT-treated WT or Langerin.DTR mice (Supporting Information Fig. 2D). Together, these data suggest that the loss of CD11c$^+$ cells drives expansion of monocytes and neutrophils in the spleen of CD11c.DTR mice. These observations agree with other published studies that have reported monocytosis and neutrophilia after depletion of DCs in other, more specific, models of DC depletion [27, 28, 31, 32]. In particular, depletion of DCs, but not macrophages, results in monocytosis in zDC.DTR mice [27]. Therefore, together these studies strongly suggest that the loss of DCs is sufficient to drive expansion of myeloid cells in these mice.

To compare monocytes from PBS- or DT-injected mice, we initially examined the cells by microscopy. Ly6C$^+$ monocytes in DT-injected mice were more vacuolated than monocytes from PBS-injected controls, suggesting that the depletion of DCs results in the expansion of a more differentiated cell (Fig. 2A). Therefore, we analyzed features associated with monocyte differentiation in vivo. Figure 2B shows that Ly6C$^+$ monocytes from DT-injected mice were more granular (increased SSC) than cells from control mice. Both populations expressed low-to-negative levels of CD11c, MHC II, and F4/80 as described for Ly6C$^+$ monocytes [33], although F4/80 was slightly increased on monocytes from DT-treated mice compared with isotype controls. However, the IgG receptor FcγRI (CD64) was expressed in both groups and the level of expression was doubled on DT-Ly6C$^+$ cells (Fig. 2C, mean expression on PBS cells = 897.4 ± 59.38 (SEM) compared with 1805 ±108.8 on DT-Ly6C$^+$ cells). Circulating Ly6C$^+$ cells in the blood of DT-injected mice also expressed higher levels of CD64 than PBS-treated controls (Fig. 2D), but these levels were lower than on Ly6C$^+$ monocytes in the spleen (Fig. 2E). Injection of DT did not lead to an increase in tissue monocytes, which expressed the highest levels of CD64 as previously reported (Supporting Information Fig. 3) [20]. Collectively, our data demonstrate that the depletion of DCs results in the accumulation of a distinct population of CD64$^+$ Ly6C$^+$ cells.

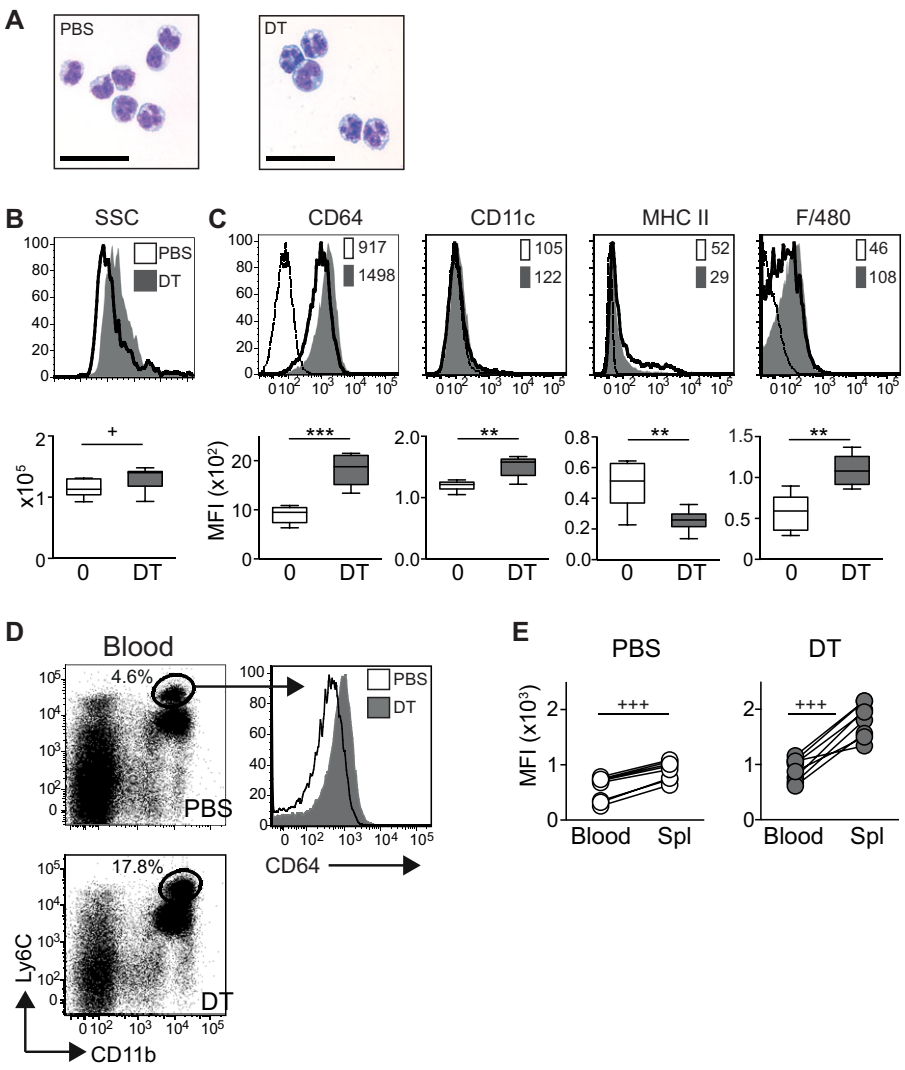

Figure 2. DT-Ly6C$^+$ monocytes express CD64. (A) Photomicrographs show Giemsa-stained cytospins of sorted CD11b$^+$Ly6C^{high}CD115^{high} cells from PBS- and DT-treated mice, bars = 100 μM. (B) Representative histograms (top) and graph (bottom) showing SSC of CD11b$^+$Ly6C^{high}CD115^{high} monocytes from PBS-treated (white) or DT-treated (gray) mice. Graph shows SSC ± SEM from PBS-treated (n = 15) and DT-treated (n = 13) mice. Data are pooled from four independent experiments: PBS versus DT p = 0.0186. (C) Top: representative histograms showing expression of labeled surface markers on CD11b$^+$Ly6C^{high} or CD11b$^+$Ly6C^{high}CD115^{high} monocytes from PBS-treated (white) and DT-treated (gray) mice. Staining with the relevant isotype control is shown by the thin line. Numbers are the median fluorescence intensity (MFI). Bottom: Graphs show the MFI ± SEM for CD64, CD11c, MHC II, and F4/80 on monocytes gated as for the histograms (n = 8 or 6 for F4/80 expression). Horizontal lines mark the mean; data are pooled from three independent experiments: CD64 PBS versus DT p = 0.0002, CD11c p = 0.0014, MHC II p = 0.0070, F4/80 p = 0.0043. (D) Left: representative dot plots showing the frequency of gated live cells in the blood of CD11c.DTR mice injected with DT 48 h earlier. Right: histograms showing expression of CD64 by CD11b$^+$Ly6C^{high} monocytes from PBS-treated (white) and DT-treated (gray) mice. (E) Paired line graphs showing the median fluorescent intensity of CD64 on CD11b$^+$Ly6C^{high} monocytes from the blood and spleens of PBS- and DT-treated mice. Data are pooled from three independent experiments, n = 8. Student's paired t-test in both PBS- and DT-treated animals, $p < 0.0001$. Statistical analyses for other experiments were carried out with a Student's unpaired t-test (+) or Mann–Whitney (*) as appropriate.

DC depletion drives expansion of a transcriptionally distinct population of Ly6C$^+$ monocytes

Ly6C$^+$ MHC class II$^+$ blood monocytes were recently identified that seed tissue monocyte populations in the steady state [19]. These cells upregulate CD64 and follow extravasation. Therefore, we examined the relationship between DT-Ly6C$^+$ monocytes and other splenic and tissue monocyte populations in more detail. We sorted test and control cell populations to high purity and compared their transcriptional profiles by hybridization to an Affymetrix microarray. Specifically, we purified spleen lineage^{neg}CD11b$^+$CD115^{high}Ly6C^{high} monocytes from DT- or PBS-injected CD11c.DTR mice, spleen lineage^{neg}CD11b$^+$CD115^{high}Ly6C^{neg} monocytes, and BM cMoPs (lineage^{neg}CD117$^+$CD115$^+$CD135^{neg}Ly6C$^+$CD11b^{neg}) [9]. All control populations were validated against publically available Immgen datasets (http://www.immgen.org, see materials and methods). Multidimensional scaling analysis, which offers a visual representation of the proximity of the datasets, demonstrated that DT-Ly6C$^+$ monocytes were transcriptionally distinct from classical Ly6C$^+$ and Ly6C^{neg} monocytes, and were more distant from precursor cells than both these populations, suggesting the development of a more differentiated cell type (Fig. 3A). To explore the lineage relationship between PBS- and DT-Ly6C$^+$ monocytes further, we specifically analyzed the expression of a panel of genes that encode transcriptional factors implicated in monocyte differentiation [3, 9]. The heat map in Figure 3B shows the relative expression of the panel of genes by macrophage/DC precursors (MDPs), cMoPs, and Ly6C$^+$ monocytes from PBS- and DT-treated mice. These data demonstrate that DT-Ly6C$^+$ monocytes express transcription factors associated with monocyte differentiation at higher levels than the other cell populations, reinforcing the concept that the depletion of DCs drives the expansion of a highly differentiated monocyte population.

DT-Ly6C$^+$ cells were transcriptionally distinct from classical splenic Ly6C$^+$ monocytes and showed features linked to more advanced differentiation, therefore, we next queried whether they were instead more similar to tissue monocytes. Thus, we

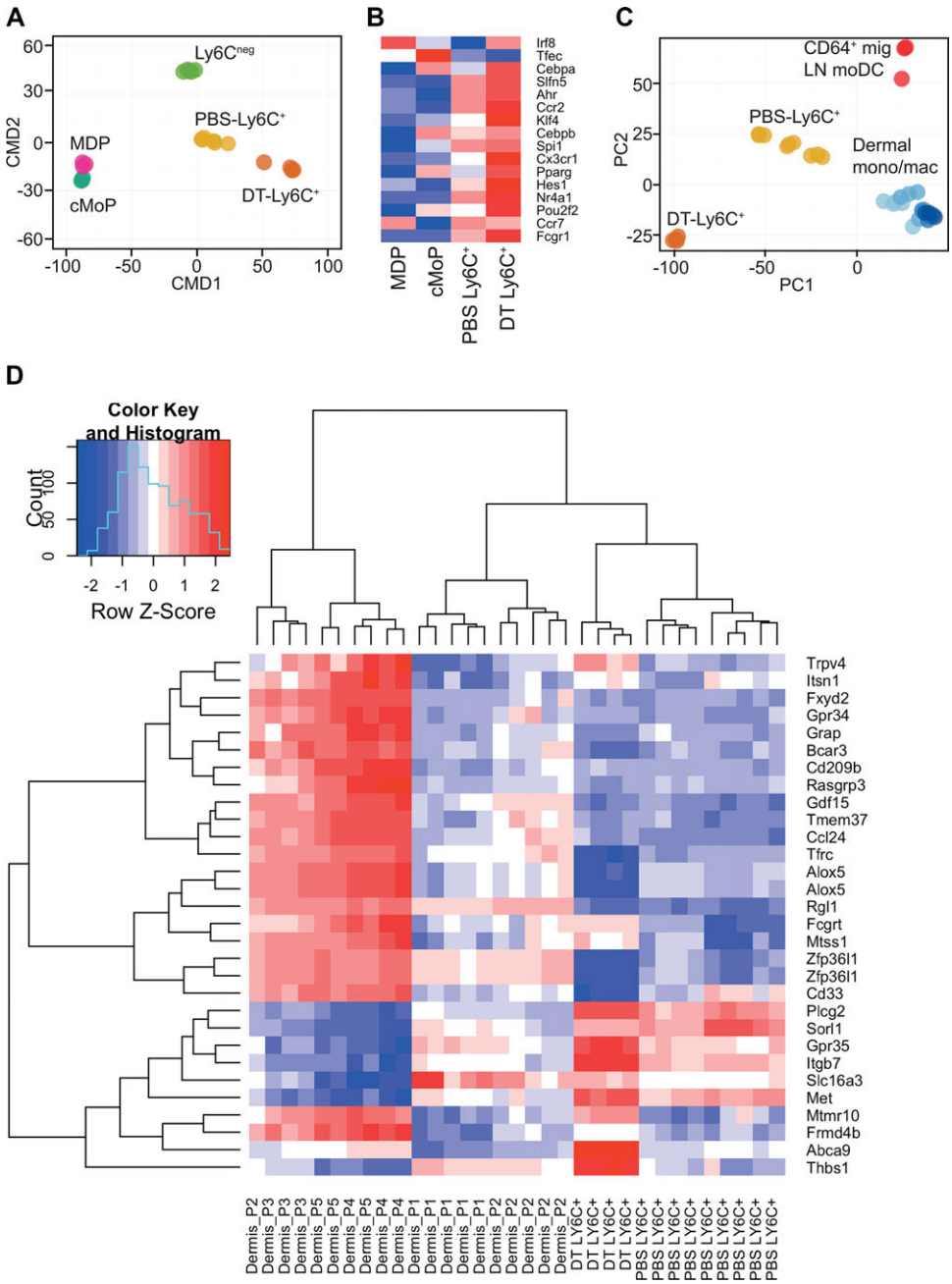

Figure 3. DT-Ly6C$^+$ monocytes are transcriptionally distinct from blood and tissue monocyte populations. CD11c.DTR mice were injected with PBS or DT, and 48 h later splenic lineage^{neg}CD11b$^+$CD115^{high}Ly6C^{high} monocytes were sorted to high purity and analyzed by hybridization to an Affymetrix microarray. We also sorted lineage^{neg}CD11b$^+$CD115^{high}Ly6C^{neg} monocytes and BM cMoPs (lineage^{neg}CD117$^+$CD115$^+$CD135^{neg}Ly6C$^+$CD11b^{neg}) from C57BL/6 mice. (A) Multidimensional Scaling (MDS) comparing the transcriptional profile of DT-Ly6C$^+$ cells to other precursors and monocyte populations (Immgen MDP $n = 3$, UCL cMoP $n = 3$, UCL PBS Ly6C$^+$ $n = 4$, and Immgen (PBS) Ly6C$^+$ $n = 3$, UCL Ly6C^{neg} $n = 3$, and Immgen $n = 2$). Each subset of cells was purified from at least two independent experiments and was derived from individual mice, or pooled from multiple mice. (B) Heat map comparing the relative expression of a panel of genes associated with monocyte differentiation in the different cell populations. (C) PCA of gene expression by DT- and PBS-Ly6C$^+$ monocytes in comparison to published data for CD64$^+$ migrating LN monocyte-derived DCs and dermal-cell subsets [20]. Approximately, 45 and 13% of the variance within the expression data is orthogonal to PC1 and PC2, respectively (58% cumulative). (D) Heat map depicting the relative expression across all samples of the principal gene signature (PC1, Supporting Information Fig. 2D) that separates the dermal P1–P5 group. DT-Ly6C$^+$ $n = 4$, PBS-Ly6C$^+$ $n = 9$ (Immgen, UCL), P1–P5 [20].

compared PBS- and DT-Ly6C$^+$ cells with the CD24^{neg} dermal monocyte/macrophage populations and migrating LN CD64$^+$ monocyte-derived DCs that can be distinguished on the basis of surface expression of CD64 and MHC Class II (P1–P5) as recently published by Tamoutounour et al. [20]. The principal components analysis (PCA) shown in Figure 3C demonstrates that extravasation of Ly6C$^+$ monocytes, and differentiation into tissue macrophages, results in the expression of a shared transcriptional profile that was not expressed by either PBS-Ly6C$^+$ or DT-Ly6C$^+$ monocytes from the spleen. However, DT-Ly6C$^+$ monocytes were clearly also distinct from PBS-Ly6C$^+$ monocytes according to both principal components 1 and 2. To focus more closely on the differences between the cell types, we examined the signatures that differentiate P1-P5 cells, again using PCA (Supporting Information Fig. 4). Then, using the strongest signature of difference within P1–P5 (the primary principal component PC1) we defined a gene signature that best distinguishes P1/2 from P3–P5. Using this signature, we plotted a heat map displaying this signature across P1-P5 and DT-Ly6C$^+$ monocytes (Fig. 3D). The heat map shows that, despite increased expression of CD64, DT-Ly6C$^+$ monocytes cluster as a true variant of Ly6C$^+$ monocytes and both populations are transcriptionally distinct from cells that have exited the vasculature and entered the tissues. However, consistent with our phenotypic analyzes, DT-Ly6C$^+$ monocytes are most similar to the P1/P2 cells of the dermal populations, that is, cells that have recently entered the skin. Of the signature genes that differentiate P1/2 dermal monocytes, DT-Ly6C$^+$ cells have upregulated higher levels of expression of a number of genes associated with cell migration and angiogenesis (*Gpr35*, *Itgb7*, *Met*, *Thbs1* [34–37]), but significantly downregulated *Cd33*, which has been shown to repress monocyte-derived pro-inflammatory cytokines [38]. Thus, our phenotypic and transcriptional profiling data show that the depletion of DCs promotes the expansion of differentiated monocytes that have upregulated expression of CD64, but that remain transcriptionally distinct from tissue monocytes, and are a true variant of splenic classical Ly6C$^+$ cells.

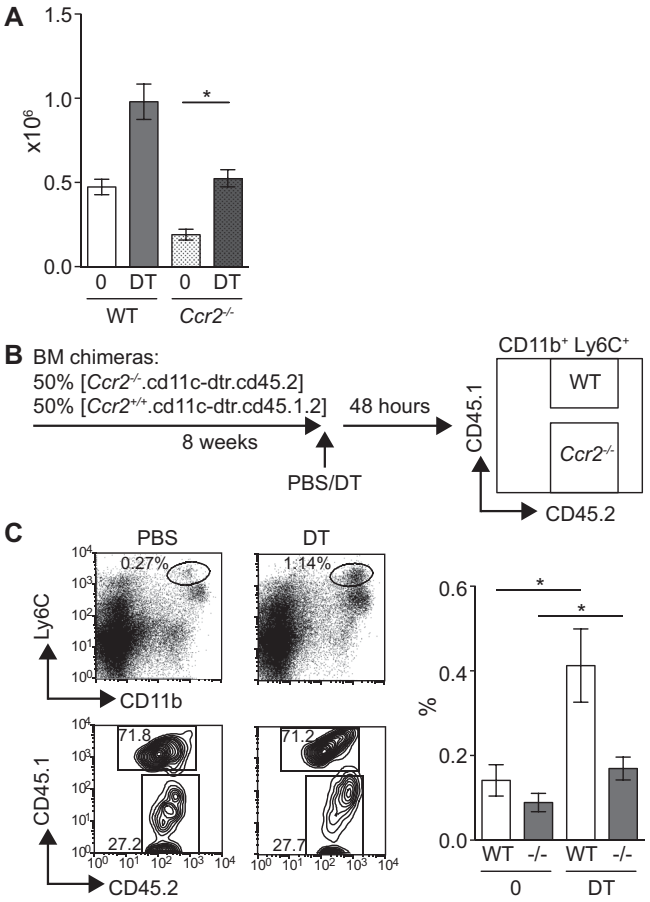

Figure 4. CCR2-independent expansion of DT-Ly6C$^+$ monocytes in vivo. (A) CD11c.DTR.Ccr2$^{-/-}$ mice or CD11c.DTR controls were injected with PBS ($n = 3$–4) or DT ($n = 2$–4) and the expansion of monocytes analyzed in the spleen 48 h later. Graph shows the number of CD11b$^+$Ly6C$^+$ cells ± SEM, PBS versus DT in CD11c.DTR.Ccr2$^{-/-}$ mice $p = 0.029$. Data are pooled from three independent experiments. (B) Schematic diagram describing the competitive chimera experiments. (C) Left: representative flow cytometry plots showing CD11b$^+$Ly6C$^+$ monocytes in pregated bulk splenic CD45.2$^+$ hematopoietic cells from PBS- or DT-treated chimeras, and the percentage of WT (CD45.1$^+$CD45.2$^+$) or Ccr2$^{-/-}$ (CD45.2$^+$) cells in the monocyte gate. Right: graph shows the frequency of WT or Ccr2$^{-/-}$ CD11b$^+$Ly6C$^+$ cells in the spleens of PBS- or DT-treated chimeras; PBS-treated ($n = 6$) and DT-treated ($n = 6$) mice. WT cells PBS versus DT $p = 0.0260$, Ccr2$^{-/-}$ cells $p = 0.0411$. Data are pooled from two independent experiments. Statistical analyses were carried out with a Mann–Whitney *U* test.

Expansion of Ly6C$^+$ monocytes in DC-depleted mice does not require signaling via CCR2

Classical Ly6C$^+$ monocytes differentiate from committed precursors in the BM before egress into the blood. Injection of DT increased the frequency of Ly6C$^+$ monocytes in the BM, whereas the frequency of macrophage/DC precursors (MDPs) or cMoPs was unchanged (Fig. 1 and Supporting Information Fig. 5A). To determine whether splenic Ly6C$^+$ monocytes were directly recruited from the BM, we initially analyzed the expansion of monocytes in mice lacking CCR2. In these mice, monocytes cannot efficiently leave the BM and *Ccr2*$^{-/-}$ animals have decreased numbers of Ly6C$^+$ monocytes in the circulation [7, 39]. Figure 4A shows that the injection of DT into *Ccr2*$^{-/-}$.CD11c.DTR mice resulted in an expansion of splenic Ly6C$^+$ monocytes to a similar extent as *Ccr2*$^{+/+}$.CD11c.DTR controls (Fig. 4A: *Ccr2*$^{+/+}$.CD11c.DTR PBS- compared to DT-injected mice = 2.1-fold mean increase in the frequency of CD11b$^+$Ly6C$^+$ monocytes; *Ccr2*$^{-/-}$.CD11c.DTR PBS- versus DT-treated = 2.7-fold increase), despite a lack of circulating monocytes in the blood (Supporting Information Fig. 5B). To directly compare the contribution of cells that could or could not signal via CCR2 to monocytosis in DT-treated mice, we adopted a mixed chimera approach [39, 40]. CD11c.DTR.CD45.1 recipients were lethally irradiated and reconstituted with an equal mixture of BM cells isolated from *Ccr2*$^{-/-}$.CD11c.DTR.CD45.2 or *Ccr2*$^{+/+}$.CD11cDTR.CD45.1.2 donors. Eight weeks later, chimeras were injected with DT, and expansion of *Ccr2*$^{-/-}$ (CD45.2)

versus WT (CD45.1.2) CD11b$^+$Ly6C$^+$ monocytes compared in the blood and spleen (Fig. 4B). As expected, Ly6C$^+$ monocytes derived from WT BM preferentially accumulated in the spleen of both PBS- and DT-treated chimeras, but with a significant contribution from *Ccr2*$^{-/-}$ cells reflecting the mix of blood-derived and extramedullary monocytes at this site [41]. Figure 4C shows that DT treatment of mixed chimeras induced expansion of both WT and *Ccr2*$^{-/-}$ Ly6C$^+$ monocytes in the spleen (2.9-fold increase in WT cells on injection of DT compared with 1.9-fold increase in *Ccr2*$^{-/-}$ cells). Together, these data show that the depletion of DCs results in the CCR2-independent expansion of some Ly6C$^+$ monocytes in the spleen, suggesting that these cells are not recruited from the BM.

Depletion of DC results in the G-CSF-dependent expansion of Ly6C$^+$ monocytes

It has been previously reported that the depletion of DCs results in increased serum levels of G-CSF [26, 31]. To test whether G-CSF was required for the expansion of monocytes in DC-depleted mice, we injected CD11c.DTR mice with αG-CSF neutralizing antibodies prior to injection of PBS or DT. Figure 5A and B demonstrates that endogenous G-CSF was required for the expansion of DT-Ly6C$^+$ monocytes and Ly6G$^+$ neutrophils in the spleen of DC-depleted mice. Consistent with the hypothesis that an increase in serum growth factors promotes the expansion of splenic monocytes in DC-depleted animals [23], subcutaneous treatment of non-DC-depleted WT mice with exogenous G-CSF also mobilized splenic monocytes and neutrophils but did not lead to an increase in the numbers of these cells in the BM (Fig. 5C; number of CD11b$^+$Ly6C^{high}Ly6G^{neg} monocytes in the BM of PBS-treated mice $= 1.28 \times 10^6 \pm 0.1376 \times 10^6$ (SEM) compared with $0.89 \times 10^6 \pm 0.09712 \times 10^6$ in G-CSF-treated mice, $n = 8$ mice per group in two independent experiments). Ly6C^{high} monocytes isolated from the spleens of G-CSF-treated mice were transcriptionally indistinguishable from DT-Ly6C$^+$ monocytes, when comparing a panel of genes with the topmost significant expression differences between PBS- and DT-Ly6C$^+$ cells (Fig. 5D).

It has been recently shown that murine neutrophils can transdifferentiate into monocytes in vivo [42, 43]. Therefore, we questioned whether DT-Ly6C$^+$ monocytes were differentiating from the enlarged neutrophil population in DC-depleted mice. To address this question, we analyzed the expression profile of a panel of signature neutrophil- and monocyte-associated genes in DT-Ly6C$^+$ monocytes [43]. The heat map in Figure 5E shows that DT-Ly6C$^+$ cells expressed a gene signature consistent with monocytic cells (e.g., *mafB*, *csf1r*), and did not express neutrophil-associated genes (e.g., *gfi1*). Despite the requirement for G-CSF shown in Figure 5A, these analyses revealed that DT-Ly6C$^+$ monocytes expressed relatively lower levels of the G-CSF receptor (*csfr3*) than PBS-Ly6C$^+$ cells. However, it has been previously shown that the G-CSF receptor is not required for G-CSF-dependent recruitment of neutrophils from the BM, suggesting indirect actions of G-CSF on target cells [44]. Together with published data, these results suggest that increases in serum G-CSF are sufficient to drive the expansion of Ly6C$^+$ monocytes in DC-depleted mice [26].

Depletion of DC results in the accumulation Ly6C$^+$ monocytes poised for innate immune activation

The effector function of Ly6C$^+$ monocytes induced in the absence of DCs is likely to depend on the immune environment encountered at the time of expansion. Therefore, to understand the environmental cues to which DT-Ly6C$^+$ monocytes might respond, we performed a gene set enrichment analysis with curated gene sets to compare the pathways of differentially expressed genes in monocytes from control or DC-depleted mice. DT-Ly6C$^+$ monocytes were enriched for genes involved in TLR and innate signaling pathways compared with control cells, with several overlapping gene sets. The two highest-ranking pathways according to the normalized enrichment score are shown in Figure 6A. Figure 6B lists the genes that contribute to the leading-edge subset of the two pathways. In addition to genes specific for the response to LPS and TLR signaling pathways (*tlr* genes, *Ly86*, *CD180*, *Peli*), DT-Ly6C$^+$ monocytes were also enriched for genes encoding proteins required for the production of cytokines involved in innate pro-inflammatory immune responses (*irf* genes, *Ikbk*, *Nfkb2*, *Zbp1*). Therefore, we hypothesized that Ly6C$^+$ monocytes from DC-depleted mice would produce more inflammatory cytokines in response to LPS, than control cells. To test this hypothesis, we analyzed the production of several cytokines by sorted Ly6C$^+$ monocytes from DC-depleted and DC-replete mice. Figure 6B shows that DT-Ly6C$^+$ monocytes produced significantly more TNF-α than classical splenic Ly6C$^+$ monocytes, while no significant differences were observed for the other cytokines tested. Together, these data support a model in which the depletion of DC leads to the accumulation of a differentiated population of monocytes that are poised for innate immune activation.

Discussion

Over the last decade, the CD11c.DTR mice and other DC depletion models have provided a powerful tool to understand DC function [1, 2, 45], but the consequences of loss of DCs on other cells of the MPS have not been fully appreciated. In this study, we have characterized the splenic monocyte population that expands after the depletion of DCs from CD11c.DTR mice. We have shown that the loss of CD11c$^+$ cells drives the accumulation of a variant population of CD64$^+$Ly6C$^+$ monocytes that upregulates the apparatus used for innate immune and TLR signaling.

Classical monocytes express high levels of Ly6C, and low levels of CD64 and MHC class II in the blood [19, 33]. Activation and/or extravasation into tissues results in the downregulation of Ly6C and upregulation of CD64 and MHC class II, resulting in a "cascade" of cells when these antigens are plotted on flow cytometric

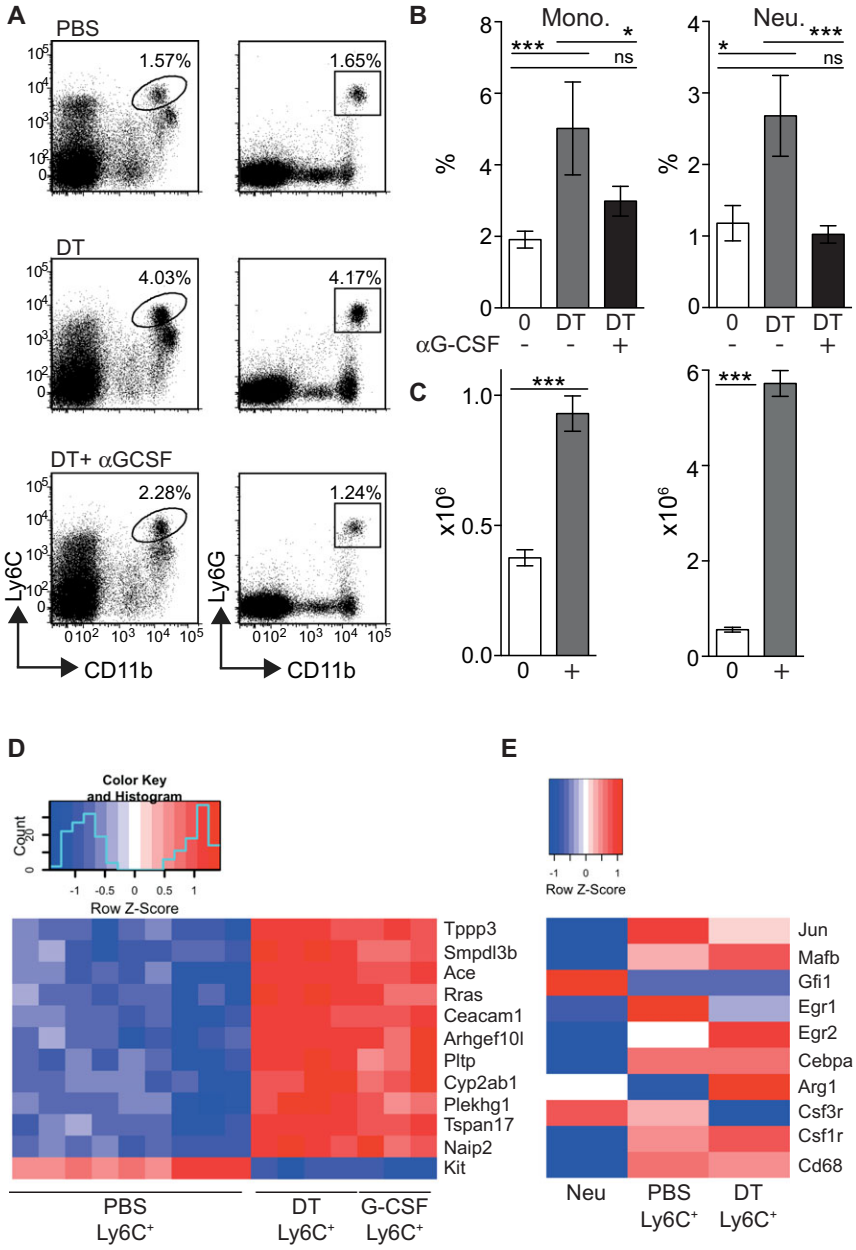

Figure 5. DC-dependent monocytosis requires G-CSF. (A) CD11c.DTR mice were injected with αG-CSF or control prior to the depletion of DCs and analyzed 48 h later. Representative dot plots showing the frequency of gated monocytes or neutrophils in the spleen. Dot plots are pregated on live single cells. (B) Graphs showing the percentage ± SEM of $CD11b^+Ly6C^{high}$ monocytes (top) or $CD11b^+Ly6G^+$ neutrophils (bottom) in the spleen and blood of PBS-treated ($n = 8$), DT + control-treated ($n = 9$), and DT + αG-CSF-treated groups ($n = 12$). Splenic monocytes PBS versus DT $p < 0.001$, DT versus DT + αG-CSF $p = 0.033$, PBS versus DT + αG-CSF $p = 0.132$; splenic neutrophils PBS versus DT $p = 0.028$, DT versus DT + αG-CSF $p < 0.001$, PBS versus DT + αG-CSF $p = 0.296$; ns = not significant. Data are pooled from three independent experiments. (C) WT mice were injected s.c. with PBS (0) or G-CSF (+) for 5 days. Graphs show the number ± SEM of $CD11b^+Ly6C^+$ monocytes (left) and $CD11b^+Ly6G^+$ neutrophils (right) in the spleens of treated or control mice. Cells were gated from plots equivalent to those shown in Figure 1A. Monocytes and neutrophils PBS versus G-CSF $p < 0.0001$. Statistical analyses were carried out with a Mann–Whitney *U* test. (D) Splenic $lineage^{neg}CD11b^+Ly6C^+$ monocytes were purified from mice treated with G-CSF (G-CSF-$Ly6C^+$ cells). A representative panel of the 12 most significant expression differences between PBS $Ly6C^+$ and DT $Ly6C^+$ monocytes was elected using the limma procedure. The heat map shows that the G-CSF $Ly6C^+$ samples show a strongly similar expression pattern to DT $Ly6C^+$ according to these genes: PBS-$Ly6C^+$ $n = 9$, DT-$Ly6C^+$ $n = 4$, G-CSF-$Ly6C^+$ $n = 3$. (E) Heat map showing differential *Z*-scored expression of a neutrophil/monocyte gene panel in the three sets of samples: Neu ($n = 4$), PBS $Ly6C^+$ ($n = 9$), and DT $Ly6C^+$ ($n = 4$). The gene expression profile for neutrophils was obtained from the Immgen database.

dot plots [20, 33, 40, 46]. This phenotypic transition as monocytes egress out of the vasculature is associated with the expression of a distinct tissue-dependent transcriptional signature (Fig. 2) [20]. Here, we have identified a population of splenic monocytes that spontaneously express CD64, but that do not cluster with dermal monocytes in PCA. Therefore, the loss of DCs results in the expansion of a variant $Ly6C^+$ splenic monocyte. However, DT-$Ly6C^+$ cells also display characteristics associated with $Ly6C^{neg}$ monocytes—for example, the upregulation of the transcription factor *Nr4a1* [47], and expression of TLRs and other molecules required for sensing of nucleic acids [5]. Our findings therefore demonstrate that the distinction between individual monocyte populations may become blurred under conditions of acute depletion of $CD11c^+$ myeloid cells when the cellular composition within the MPS is perturbed.

Recent publications have presented an emerging picture of control of homeostasis within the MPS by serum cytokines, notably M-CSF. Removal of populations that bind these cytokines will result in a decrease in the local concentration, which may impact on the proliferation and survival of other myeloid populations [10, 48]. DC populations act as a cellular sink for the growth factors G-CSF and Flt3(L) [25, 26]. We have shown that G-CSF is required for the expansion of splenic monocytes after the loss of DCs, and that exogenous G-CSF is sufficient to induce a variant monopoiesis that is similar to that seen in DC-depleted mice. Depletion of DCs also induces the expansion of splenic neutrophils that are functionally important for the clearance of bacterial infections in these models [26, 30]. Jiao et al. recent reported that the depletion of DCs from CD11c.DTR mice leads to neutrophilia in the spleen and tissues by enhancing recruitment out of the BM

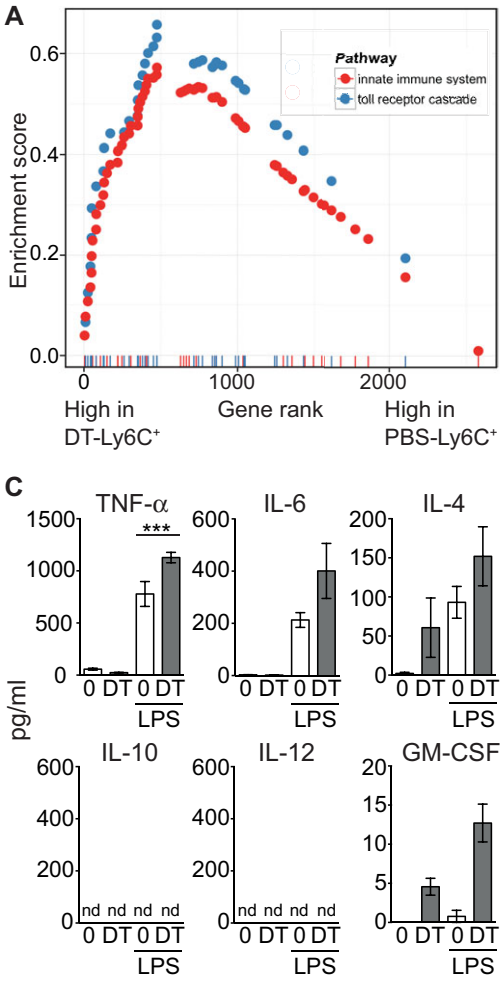

Toll receptor cascade	Innate immune system	
Ly86	*Cfb*	*Map3k1*
Tlr9	*Ly86*	*Ccr2*
Tlr7	*Tlr9*	*Tlr8*
Ctss	*Tlr7*	*Peli1*
Irf7	*Ctss*	*Nfkb2*
Cd180	*Irf7*	*Irf2*
Dusp3	*Pros1*	*Mef2c*
Ripk2	*Cd180*	*Fos*
Lgmn	*Zbp1*	*Ifih1*
Ikbkb	*P2rx7*	*Mef2a*
Map3k1	*Dusp3*	*Ctsb*
Tlr8	*Ripk2*	*Ly96*
Peli1	*Ube216*	*Irak3*
Nfkb2	*Lgmn*	
Mef2a	*Cfh*	
Ctsb	*Isg15*	
Ly96	*Lgals3*	
Irak3	*Ikbkb*	

Figure 6. DT-Ly6C$^+$ monocytes express genes associated with innate immune activation, and secrete high levels of TNF-α upon stimulation with LPS. (A) Gene set enrichment analysis was used to identify differentially expressed pathways between DT-Ly6C$^+$ cells and their most closely related group: PBS-Ly6C$^+$. The rank-versus-ES score plots are shown for two representative pathways upregulated in DT-Ly6C$^+$ cells: blue = Reactome toll receptor cascade, red = Reactome innate immune system. All pathways were significantly altered (false discovery rate q-values < 0.01). (B) Table showing the core enriched genes for the two pathways. (C) Purified CD11b$^+$Ly6C$^+$CD115^{high} monocytes from PBS-treated ($n = 6$) or DT-treated ($n = 6$) treated mice were cultured overnight in medium with or without LPS. Graphs show the amount ± SEM of cytokines secreted into the culture supernatant. TNF-α PBS versus DT for LPS-treated cells, $p = 0.022$. Data are pooled from two independent experiments. Statistical analyses were carried out with a Student's unpaired t-test.

[31]. We have shown that monocytes and neutrophils expand concurrently in the spleen after depletion of CD11c$^+$ cells, and both populations expand in response to G-CSF. It is not possible however to infer causative mechanisms from these studies, and future work is needed to determine whether G-CSF has a direct or indirect effect on the expansion of monocytes in this model. Our data further demonstrate that cells that do not express CCR2 expand in the spleens of DT-treated recipients. While we cannot exclude a contribution from BM-derived cells, these data strongly support a role for extramedullary expansion of monocytes or their precursors. We did not detect differences in proliferation of Ly6C$^+$ cells in the spleens of PBS- or DT-treated mice 48 h after treatment (data not shown), however it is possible that we missed the point of proliferation in our experiments. In addition, loss of CD11c$^+$ cells may lead to local proliferation of splenic monocyte precursors, including cMoPs [9]. Our findings are in line with previous data showing that constitutive ablation of DCs resulted in monocytosis due to a direct increase in hematopoiesis in the spleen [23].

Expression of CD11c is not restricted to DCs, and other cell types may be depleted from CD11c.DTR mice [29, 49, 50]. We did not observe changes in lymphoid cell populations in our model, but F4/80$^+$ macrophages were absent from the spleen 48 h after injection of DT. Removal of macrophages will lead to increases in serum M-CSF which could modulate monocyte populations [48]. However, the depletion of DCs results in the expansion of monocytes and neutrophils in other mouse models in which DC populations are specifically perturbed, strongly suggesting that monocytosis in the CD11c.DTR mice is directly dependent on the ablation of DCs [27, 31].

In conclusion we have shown that removal of CD11c$^+$ cells from the MPS in the steady state is sufficient to drive the rapid transient expansion of a differentiated population of monocytes in the spleen, suggesting a model in which the loss of DCs drives the expansion of an effector monocyte population. Our kinetic analyses suggest a transient peak in the accumulation of splenic monocytes in DC-depleted mice. Therefore, there is a defined window in DT-injected mice in which DT-Ly6C$^+$ monocytes may mediate responses to infectious or inflammatory challenge in the absence of DCs. These cells may be sensitive to the environment in which they emerge and, consistent with this concept, we have recently demonstrated that monocytes mobilized by injection of G-CSF produce iNOS, and become immunosuppressive, in a murine model of GVH disease [51].

It has been recently demonstrated that expression of the high-affinity DTR by DCs leads to hypocellularity in LN, but not in the spleen of CD11c.DTR mice [32]. Together with our data, this study

highlights the caution with which DC-depletion studies should be interpreted, particularly in the context of infection and/or inflammation.

Materials and methods

Mice

Animal protocols were approved by local institutional research committees and in accordance with U.K. Home Office guidelines. CD11c.DTR/GFP (B6.FVB-Tg(Itgax-DTR/ EGFP)57Lan/J) were used as both heterozygotes and homozygotes for the DTR/GFP transgene [52]. *Ccr2*$^{-/-}$ mice were a kind gift from Frederic Geissmann [39]. CD11c^{+} DCs were depleted by a single i.p. injection of 100 ng of DT (Sigma, UK) in PBS [52, 53]. Depletion of DCs was confirmed in all experiments. To mobilize Ly6C^{+} monocytes C57BL/6 mice were injected s.c. for 5 days with rhuman G-CSF (200 μg/kg/day; Neupogen, Amgen, France) or PBS vehicle. G-CSF was neutralized by i.p. injection of two doses of 50 μg αG-CSF 24 h apart (Clone 67604, R&D Systems U.K.) adapted from published data [54]. Controls received either nonspecific IgG1 or PBS. The second dose was given immediately prior to the injection of PBS or DT.

Competitive chimeras

Ten-week-old C57BL/6 mice received 11Gy X-ray irradiation before i.v. injection of a 1:1 mixture of CD11c.DTR.CD45.1.CD45.2 and CD11c.DTR.*Ccr2*$^{-/-}$.CD45.2 BM cells (5 × 10^{6} total cells). Chimeric mice were used at ~3 months post reconstitution.

Flow cytometry

Spleens were digested with Collagenase IV (Worthington Biochemical Corporation). The following antibodies were used for flow cytometric analysis, all from eBiosciences or BD-Biosciences: FcBlock (clone 2.4G2), anti-CD11b (M1/70), anti-CD11c (HL3), anti-Ly-6C (AL-21), anti-Ly-6G (1A8), anti-CD45.1 (A20), anti-CD45.2 (104), anti-MHCII (M5/114.15.2), anti-CD115 (AFS98), anti-CD64, anti-F4/80 (BM8), anti-CD135 (A2F10), anti-CD117 (2B8). FSC-W and a lineage dump gate were used in some experiments to exclude irrelevant cells (anti-CD3 (145-2C11), anti-CD19 (1D3), anti-B220 (RA3-6B2), anti-NK-1.1 (PK136), and anti-Ly-6G (1A8)). Samples were acquired using a BD LSR Fortessa Cell Analyzer (BD Bioscience), and analyzed using FlowJo software (Treestar).

Microscopy

Splenic CD11b^{+}Ly6C^{+} cells were FACS-sorted and spun onto slides using a Cytospin 2 Centrifuge (Shandon Instruments). The cells were air-dried, fixed with methanol, and stained with Giemsa (Sigma Aldrich). Images were acquired using a Leica DMD108 (Leica Microsystems) microscope.

Microarray analysis, normalization, and validation

Total RNA was extracted from sorted cells using the RNeasy Microkit (Qiagen, UK) and hybridized on Affymetrix Mogene 2.0 arrays at the UCL Cancer Institute core facility. A detailed description of the methods used is included in the Supporting Information.

Luminex

Sorted monocytes were cultured for 12 h ± 100 ng/mL LPS (Sigma-Aldrich) at 2.5 × 10^{5} cells/mL in duplicate wells, and the supernatant analyzed with the FIDIS system using Luminex 100 software (LuminexCorp) and Mouse cytokine 10-plex panel (Life Technologies).

Statistical analysis

Data were analyzed using Graphpad Prism 6 and statistical comparisons were made by using a two-tailed Student *t*-test for parametric data and a two-tailed Mann–Whitney *U* test for non-parametric data. The kinetic experiments were analyzed using a two-way ANOVA with multiple comparisons at different time points, and an adjusted p-value according to Sidak's multiple-comparison test.

Acknowledgements: The authors thank the members of the Bennett and Chakraverty labs for their helpful discussions of this work. This study was supported by research funding from Leukaemia and Lymphoma Research, UK, to S.S., S.W., T.M., L.Z., R.C. and C.L.B. (grants 10007 and 12006) and from the APHP (Assistance Publique–Hôpitaux de Paris, France), Cancéropôle d'Ile de France, and the Institut National du Cancer, Paris, France, to M.D., O.H., and M.-T.R.

Conflict of interest: The authors declare no financial or commercial conflict of interest.

References

1 **Bennett, C. L. and Clausen, B. E.**, DC ablation in mice: promises, pitfalls, and challenges. *Trends Immunol.* 2007. **28**: 525–531.

2 **van Blijswijk, J., Schraml, B. U. and Reis e Sousa, C.**, Advantages and limitations of mouse models to deplete dendritic cells. *Eur. J. Immunol.* 2013. **43**: 22–26.

3 **Geissmann, F., Manz, M. G., Jung, S., Sieweke, M. H., Merad, M. and Ley, K.**, Development of monocytes, macrophages, and dendritic cells. *Science* 2010. **327**: 656–661.

4 **Ginhoux, F. and Jung, S.**, Monocytes and macrophages: developmental pathways and tissue homeostasis. *Nat. Rev. Immunol.* 2014. **14**: 392–404.

5 **Carlin, L. M., Stamatiades, E. G., Auffray, C., Hanna, R. N., Glover, L., Vizcay-Barrena, G., Hedrick, C. C. et al.**, Nr4a1-dependent Ly6C(low) monocytes monitor endothelial cells and orchestrate their disposal. *Cell* 2013. **153**: 362–375.

6 **Shi, C., Jia, T., Mendez-Ferrer, S., Hohl, T. M., Serbina, N. V., Lipuma, L., Leiner, I. et al.**, Bone marrow mesenchymal stem and progenitor cells induce monocyte emigration in response to circulating toll-like receptor ligands. *Immunity* 2011. **34**: 590–601.

7 **Serbina, N. V. and Pamer, E. G.**, Monocyte emigration from bone marrow during bacterial infection requires signals mediated by chemokine receptor CCR2. *Nat. Immunol.* 2006. **7**: 311–317.

8 **Tsou, C. L., Peters, W., Si, Y., Slaymaker, S., Aslanian, A. M., Weisberg, S. P., Mack, M. et al.**, Critical roles for CCR2 and MCP-3 in monocyte mobilization from bone marrow and recruitment to inflammatory sites. *J. Clin. Invest.* 2007. **117**: 902–909.

9 **Hettinger, J., Richards, D. M., Hansson, J., Barra, M. M., Joschko, A. C., Krijgsveld, J. and Feuerer, M.**, Origin of monocytes and macrophages in a committed progenitor. *Nat. Immunol.* 2013. **14**: 821–830.

10 **Yona, S., Kim, K. W., Wolf, Y., Mildner, A., Varol, D., Breker, M., Strauss-Ayali, D. et al.**, Fate mapping reveals origins and dynamics of monocytes and tissue macrophages under homeostasis. *Immunity* 2013. **38**: 79–91.

11 **Nakano, H., Lin, K. L., Yanagita, M., Charbonneau, C., Cook, D. N., Kakiuchi, T. and Gunn, M. D.**, Blood-derived inflammatory dendritic cells in lymph nodes stimulate acute T helper type 1 immune responses. *Nat. Immunol.* 2009. **10**: 394–402.

12 **Egawa, M., Mukai, K., Yoshikawa, S., Iki, M., Mukaida, N., Kawano, Y., Minegishi, Y. et al.**, Inflammatory monocytes recruited to allergic skin acquire an anti-inflammatory M2 phenotype via basophil-derived interleukin-4. *Immunity* 2013. **38**: 570–580.

13 **Tacke, F., Alvarez, D., Kaplan, T. J., Jakubzick, C., Spanbroek, R., Llodra, J., Garin, A. et al.**, Monocyte subsets differentially employ CCR2, CCR5, and CX3CR1 to accumulate within atherosclerotic plaques. *J. Clin. Invest.* 2007. **117**: 185–194.

14 **Goldszmid, R. S., Caspar, P., Rivollier, A., White, S., Dzutsev, A., Hieny, S., Kelsall, B. et al.**, NK cell-derived interferon-gamma orchestrates cellular dynamics and the differentiation of monocytes into dendritic cells at the site of infection. *Immunity* 2012. **36**: 1047–1059.

15 **Grainger, J. R., Wohlfert, E. A., Fuss, I. J., Bouladoux, N., Askenase, M. H., Legrand, F., Koo, L. Y. et al.**, Inflammatory monocytes regulate pathologic responses to commensals during acute gastrointestinal infection. *Nat. Med.* 2013. **19**: 713–721.

16 **Leiriao, P., del Fresno, C. and Ardavin, C.**, Monocytes as effector cells: activated Ly-6C(high) mouse monocytes migrate to the lymph nodes through the lymph and cross-present antigens to CD^{8+} T cells. *Eur. J. Immunol.* 2012. **42**: 2042–2051.

17 **Leon, B., Lopez-Bravo, M. and Ardavin, C.**, Monocyte-derived dendritic cells formed at the infection site control the induction of protective T helper 1 responses against *Leishmania*. *Immunity* 2007. **26**: 519–531.

18 **Serbina, N. V., Salazar-Mather, T. P., Biron, C. A., Kuziel, W. A. and Pamer, E. G.**, TNF/iNOS-producing dendritic cells mediate innate immune defense against bacterial infection. *Immunity* 2003. **19**: 59–70.

19 **Jakubzick, C., Gautier, E. L., Gibbings, S. L., Sojka, D. K., Schlitzer, A., Johnson, T. E., Ivanov, S. et al.**, Minimal differentiation of classical monocytes as they survey steady-state tissues and transport antigen to lymph nodes. *Immunity* 2013. **39**: 599–610.

20 **Tamoutounour, S., Guilliams, M., Montanana Sanchis, F., Liu, H., Terhorst, D., Malosse, C., Pollet, E. et al.**, Origins and functional specialization of macrophages and of conventional and monocyte-derived dendritic cells in mouse skin. *Immunity* 2013. **39**: 925–938.

21 **Bain, C. C., Scott, C. L., Uronen-Hansson, H., Gudjonsson, S., Jansson, O., Grip, O., Guilliams, M. et al.**, Resident and pro-inflammatory macrophages in the colon represent alternative context-dependent fates of the same Ly6Chi monocyte precursors. *Mucosal Immunol.* 2013. **6**: 498–510.

22 **Auffray, C., Sieweke, M. H. and Geissmann, F.**, Blood monocytes: development, heterogeneity, and relationship with dendritic cells. *Annu. Rev. Immunol.* 2009. **27**: 669–692.

23 **Birnberg, T., Bar-On, L., Sapoznikov, A., Caton, M. L., Cervantes-Barragan, L., Makia, D., Krauthgamer, R. et al.**, Lack of conventional dendritic cells is compatible with normal development and T cell homeostasis, but causes myeloid proliferative syndrome. *Immunity* 2008. **29**: 986–997.

24 **Darrasse-Jeze, G., Deroubaix, S., Mouquet, H., Victora, G. D., Eisenreich, T., Yao, K. H., Masilamani, R. F. et al.**, Feedback control of regulatory T cell homeostasis by dendritic cells in vivo. *J. Exp. Med.* 2009. **206**: 1853–1862.

25 **Liu, K., Victora, G. D., Schwickert, T. A., Guermonprez, P., Meredith, M. M., Yao, K., Chu, F. F. et al.**, In vivo analysis of dendritic cell development and homeostasis. *Science* 2009. **324**: 392–397.

26 **Autenrieth, S. E., Warnke, P., Wabnitz, G. H., Lucero Estrada, C., Pasquevich, K. A., Drechsler, D., Gunter, M. et al.**, Depletion of dendritic cells enhances innate anti-bacterial host defense through modulation of phagocyte homeostasis. *PLoS Pathog.* 2012. **8**: e1002552.

27 **Meredith, M. M., Liu, K., Darrasse-Jeze, G., Kamphorst, A. O., Schreiber, H. A., Guermonprez, P., Idoyaga, J. et al.**, Expression of the zinc finger transcription factor zDC (Zbtb46, Btbd4) defines the classical dendritic cell lineage. *J. Exp. Med.* 2012. **209**: 1153–1165.

28 **Hochweller, K., Striegler, J., Hammerling, G. J. and Garbi, N.**, A novel CD11c.DTR transgenic mouse for depletion of dendritic cells reveals their requirement for homeostatic proliferation of natural killer cells. *Eur. J. Immunol.* 2008. **38**: 2776–2783.

29 **Probst, H. C., Tschannen, K., Odermatt, B., Schwendener, R., Zinkernagel, R. M. and van den Broek, M.**, Histological analysis of CD11c-DTR/GFP mice after in vivo depletion of dendritic cells. *Clin. Exp. Immunol.* 2005. **141**: 398–404.

30 **Tittel, A. P., Heuser, C., Ohliger, C., Llanto, C., Yona, S., Hammerling, G. J., Engel, D. R. et al.**, Functionally relevant neutrophilia in CD11c diphtheria toxin receptor transgenic mice. *Nat. Methods* 2012. **9**: 385–390.

31 **Jiao, J., Dragomir, A. C., Kocabayoglu, P., Rahman, A. H., Chow, A., Hashimoto, D., Leboeuf, M. et al.**, Central role of conventional dendritic cells in regulation of bone marrow release and survival of neutrophils. *J. Immunol.* 2014. **192**: 3374–3382.

32 **van Blijswijk, J., Schraml, B. U., Rogers, N. C., Whitney, P. G., Zelenay, S., Acton, S. E. and Reis, E. S. C.**, Altered lymph node composition in diphtheria toxin receptor-based mouse models to ablate dendritic cells. *J. Immunol.* 2015. **194**: 307–315.

33 **Ingersoll, M. A., Spanbroek, R., Lottaz, C., Gautier, E. L., Frankenberger, M., Hoffmann, R., Lang, R. et al.**, Comparison of gene expression profiles between human and mouse monocyte subsets. *Blood* 2010. **115**: e10–19.

34 **Barth, M. C., Ahluwalia, N., Anderson, T. J., Hardy, G. J., Sinha, S., Alvarez-Cardona, J. A., Pruitt, I. E. et al.**, Kynurenic acid triggers firm arrest of leukocytes to vascular endothelium under flow conditions. *J. Biol. Chem.* 2009. **284**: 19189–19195.

35 **Friedl, P. and Weigelin, B.**, Interstitial leukocyte migration and immune function. *Nat. Immunol.* 2008. **9**: 960–969.

36 **Chen, Q., DeFrances, M. C. and Zarnegar, R.**, Induction of met proto-oncogene (hepatocyte growth factor receptor) expression during human monocyte-macrophage differentiation. *Cell Growth Differ.* 1996. **7**: 821–832.

37 **Carrer, A., Moimas, S., Zacchigna, S., Pattarini, L., Zentilin, L., Ruozi, G., Mano, M. et al.**, Neuropilin-1 identifies a subset of bone marrow $Gr1^-$ monocytes that can induce tumor vessel normalization and inhibit tumor growth. *Cancer Res.* 2012. **72**: 6371–6381.

38 **Lajaunias, F., Dayer, J. M. and Chizzolini, C.**, Constitutive repressor activity of CD33 on human monocytes requires sialic acid recognition and phosphoinositide 3-kinase-mediated intracellular signaling. *Eur. J. Immunol.* 2005. **35**: 243–251.

39 **Boring, L., Gosling, J., Chensue, S. W., Kunkel, S. L., Farese, R. V., Jr., Broxmeyer, H. E. and Charo, I. F.**, Impaired monocyte migration and reduced type 1 (Th1) cytokine responses in C-C chemokine receptor 2 knockout mice. *J. Clin. Invest.* 1997. **100**: 2552–2561.

40 **Langlet, C., Tamoutounour, S., Henri, S., Luche, H., Ardouin, L., Gregoire, C., Malissen, B. et al.**, CD64 expression distinguishes monocyte-derived and conventional dendritic cells and reveals their distinct role during intramuscular immunization. *J. Immunol.* 2012. **188**: 1751–1760.

41 **Swirski, F. K., Nahrendorf, M., Etzrodt, M., Wildgruber, M., Cortez-Retamozo, V., Panizzi, P., Figueiredo, J. L. et al.**, Identification of splenic reservoir monocytes and their deployment to inflammatory sites. *Science* 2009. **325**: 612–616.

42 **Araki, H., Katayama, N., Yamashita, Y., Mano, H., Fujieda, A., Usui, E., Mitani, H. et al.**, Reprogramming of human postmitotic neutrophils into macrophages by growth factors. *Blood* 2004. **103**: 2973–2980.

43 **Koffel, R., Meshcheryakova, A., Warszawska, J., Hennig, A., Wagner, K., Jorgl, A., Gubi, D. et al.**, Monocytic cell differentiation from band-stage neutrophils under inflammatory conditions via MKK6 activation. *Blood* 2014. **124**: 2713–2724.

44 **Semerad, C. L., Liu, F., Gregory, A. D., Stumpf, K. and Link, D. C.**, G-CSF is an essential regulator of neutrophil trafficking from the bone marrow to the blood. *Immunity* 2002. **17**: 413–423.

45 **Hochweller, K., Striegler, J., Hammerling, G. J. and Garbi, N.**, A novel CD11c.DTR transgenic mouse for depletion of dendritic cells reveals their requirement for homeostatic proliferation of natural killer cells. *Eur. J. Immunol.* 2008. **38**: 2776–2783.

46 **Plantinga, M., Guilliams, M., Vanheerswynghels, M., Deswarte, K., Branco-Madeira, F., Toussaint, W., Vanhoutte, L. et al.**, Conventional and monocyte-derived CD11b(+) dendritic cells initiate and maintain T helper 2 cell-mediated immunity to house dust mite allergen. *Immunity* 2013. **38**: 322–335.

47 **Hanna, R. N., Carlin, L. M., Hubbeling, H. G., Nackiewicz, D., Green, A. M., Punt, J. A., Geissmann, F. et al.**, The transcription factor NR4A1 (Nur77) controls bone marrow differentiation and the survival of Ly6C- monocytes. *Nat. Immunol.* 2011. **12**: 778–785.

48 **Jenkins, S. J. and Hume, D. A.**, Homeostasis in the mononuclear phagocyte system. *Trends Immunol.* 2014. **35**: 358–367.

49 **Iannacone, M., Moseman, E. A., Tonti, E., Bosurgi, L., Junt, T., Henrickson, S. E., Whelan, S. P. et al.**, Subcapsular sinus macrophages prevent CNS invasion on peripheral infection with a neurotropic virus. *Nature* 2010. **465**: 1079–1083.

50 **Zammit, D. J., Cauley, L. S., Pham, Q. M. and Lefrancois, L.**, Dendritic cells maximize the memory CD8 T cell response to infection. *Immunity* 2005. **22**: 561–570.

51 **D'Aveni, M., Rossignol, J., Coman, T., Sivakumaran, S., Henderson, S., Manzo, T., Santos, E. S. P. et al.**, G-CSF mobilizes CD34+ regulatory monocytes that inhibit graft-versus-host disease. *Sci. Transl. Med.* 2015. **7**: 281ra242.

52 **Goold, H. D., Escors, D., Conlan, T. J., Chakraverty, R. and Bennett, C. L.**, Conventional dendritic cells are required for the activation of helper-dependent CD8 T cell responses to a model antigen after cutaneous vaccination with lentiviral vectors. *J. Immunol.* 2011. **186**: 4565–4572.

53 **Jung, S., Unutmaz, D., Wong, P., Sano, G., de los Santos, K., Sparwasser, T., Wu, S. et al.**, In vivo depletion of CD11c(+) dendritic cells abrogates priming of CD8(+) T cells by exogenous cell-associated antigens. *Immunity* 2002. **17**: 211–220.

54 **Shojaei, F., Wu, X., Qu, X., Kowanetz, M., Yu, L., Tan, M., Meng, Y. G. et al.**, G-CSF-initiated myeloid cell mobilization and angiogenesis mediate tumor refractoriness to anti-VEGF therapy in mouse models. *Proc. Natl. Acad. Sci. USA* 2009. **106**: 6742–6747.

Abbreviations: **cMoP**: common monocyte progenitor · **DT**: diphtheria toxin · **DTR**: diphtheria toxin receptor · **Flt3(L)**: fms-like tyrosine kinase receptor-3 (ligand) · **MPS**: mononuclear phagocyte system

Full correspondence: Dr. Clare L. Bennett, Department of Haematology, Cancer Institute, University College London, Royal Free Campus, Rowland Hill Street, London NW3 2PF, UK
e-mail: c.bennett@ucl.ac.uk
Tel: +44 2077940500 x22470

Received: 7/5/2015
Revised: 10/9/2015
Accepted: 7/10/2015
Accepted article online: 14/10/2015